Helical collapse of a whirling elastic rod forced to lie on a cylinder

G.H.M. van der Heijden
Centre for Nonlinear Dynamics
University College London
London WC1E 6BT, UK

W.B. Fraser
School of Mathematics and Statistics
The University of Sydney
NSW 2006, Australia

July 1, 2001

Abstract

Extending our previous work, we apply the large-deflection rod theory to a periodically driven elastic rod in continuous contact with a cylindrical surface. Applications of this problem are found in oilwell drilling and textile yarn spinning. The previously uncovered quasi-statical helical collapse of the constrained rod is studied in the quasi-stationary context, and its occurrence examined as a function of the applied end loads and the driving frequency. Balanced plies, which are also relevant in DNA supercoiling, are shown to be special solutions of the problem under consideration.

1 Introduction

Whirling rods in a constrained environment are encountered in a variety of industrial applications, e.g., rotating drill strings confined to narrow boreholes in oilwell drilling (see, e.g., [17, 10] for recent references) and in textile yarn manufacturing processes such a two-for-one twisting where the yarn is constrained by a cylindrical guide surface [3, 4]. Here we consider the case of *quasi-stationary* rotations of a long rod in continuous contact with a cylindrical surface (i.e., the configuration of the rod is stationary when viewed in a reference frame that rotates with a constant angular velocity).

There exists an extensive literature on drill strings, both on the statics and the dynamics of the problem. Buckling problems have mostly been studied in the context of statics. The precise post-buckling behaviour is a major concern to the drilling industry as the configuration of the drill string may seriously affect the transmission of axial loads from the surface to the bit. Since the buckled drill string is confined within a relatively narrow borehole, it is in contact with the surrounding wall along most of its length. Consequently, many authors have assumed continuous contact between the drill string (either heavy or weightless) and the borehole wall. In fact, in most cases a helical shape for the drill string is assumed [16, 10]. Similarly, in yarn spinning the yarn lies on a cylindrical surface for considerable lengths. When the yarn is unwound from a stationary helically wound cylindrical package [1] it first moves away from its stationary position in the package surface until its tangent angle is just right for it to lift off the

surface and fly into a rotating loop of yarn (the so-called ring-spinning balloon) [6]. In previous work by one of us [19] the continuous-contact assumption was made but no assumption on the shape of the rod was required. Rather, all equilibrium solutions supported by the applied end loads were found (including the helical ones). An interesting feature was the collapse of the rod into a helical configuration at certain critical loads.

More on the dynamical front, synchronous whirling drill string motions have been studied by Jansen [11] in a simple beam model taking account only of the first bending vibration mode. The recent study by Tucker & Wang [17] is one of the rare cases of a full large-deflection Cosserat modelling of the dynamics of drill strings. However, their model is so inclusive (dealing, for instance, with accurate modelling of friction, drill-bit characteristics and bore cavity interactions) that the underlying mathematical features tend to get hidden away. Our work aims to occupy the middle ground.

Explicitly, this work makes three contributions. Firstly, the statics formulation developed in [19] is extended to allow for quasi-stationary rotations of a periodically driven rod. Secondly, as we shall be restricting our attention in this paper to unshearable linearly elastic rods of inextensible centreline and uniform symmetrical cross-section we take this opportunity to present the formulation of the problem using the traditional notation of engineering structural mechanics, rather than the Cosserat formulation in [19]. We hope that this will render our results in a form more accessible to a wider engineering audience. We also explore the previously uncovered quasi-statical helical collapse of the rod more carefully as a function of the physical parameters. Thirdly, we show that so-called balanced ply solutions as have recently attracted a good deal of interest in studies of yarn twisting [7, 8, 13] and DNA supercoiling [2, 14, 15] are special solutions of a rod with cylindrical constraint which occur naturally within our wider formulation.

The organisation of the paper is as follows. We start in Section 2 by giving a formulation of the more general problem of a rod moving on a cylinder, including full dynamical effects (both translational and rotary inertia), friction and the finite thickness of the rod. Next, in Section 3, a dimensional analysis is performed to assess the importance of each of these effects in a given application. It turns out that in most of the applications we are interested in only the translational inertia plays a significant role. Keeping this inertia in the equations we then study the quasi-stationary rotations in detail in Sections 4 and 5. These solutions are found as stationary solutions in a frame moving with the (constant) driving frequency. In this frame the equilibrium equations essentially reduce to the statics equations studied in [19] with just a constant centrifugal force added. The use of a cylindrical co-ordinate system allows us to eliminate the constraint and to reduce the problem to that of an equivalent planar oscillator in terms of the angle the local tangent of the rod axis makes with the axis of the cylinder. Section 6 focusses on the special balanced ply solutions, and we close this study in Section 7 with a discussion.

2 General formulation

A detailed derivation of the equations for an elastic rod of uniform circular cross-section with respect to a rotating reference frame can be found in the recent paper of Clark *et al.* [1]. The derivation in that paper applies to the yarn spinning problem and includes the effect of the rod being drawn through the system with a velocity $\mathcal{V}$ in the direction of the rod axis as the yarn

is unwound over-end from a cylindrical yarn package. In the present case $\mathcal{V} = 0$. Here we give only a summary of the derivation.

Let $\{\boldsymbol{i}, \boldsymbol{j}, \boldsymbol{k}\}$ be the basis vectors of a right-handed orthonormal co-ordinate system rotating with respect to an inertial frame with constant angular velocity ω about $\boldsymbol{k}$ which is pointing along the axis of the cylinder. We also introduce the corresponding cylindrical co-ordinates (r, θ, z) with basis vectors $(\boldsymbol{e}_r, \boldsymbol{e}_\theta, \boldsymbol{e}_z)$ given by

$$\begin{aligned} \boldsymbol{e}_r &= \cos\theta\, \boldsymbol{i} + \sin\theta\, \boldsymbol{j}, \\ \boldsymbol{e}_\theta &= -\sin\theta\, \boldsymbol{i} + \cos\theta\, \boldsymbol{j}, \\ \boldsymbol{e}_z &= \boldsymbol{k}. \end{aligned} \tag{1}$$

Thus $\boldsymbol{e}_r$ is normal to the cylinder, $\boldsymbol{e}_\theta$ in the circumferential direction, and $\boldsymbol{e}_z$ in the direction of the axis of the cylinder. The equation for the rate of change of linear momentum of the rod element a distance s along the rod axis from some reference point on the axis with position vector $\boldsymbol{R}(s,t)$ relative to the origin of the rotating reference frame at time t can now be written as

$$m\{D^2\boldsymbol{R} + 2\omega\boldsymbol{k} \times D\boldsymbol{R} + \omega^2\boldsymbol{k} \times (\boldsymbol{k} \times \boldsymbol{R})\} = (T\boldsymbol{R}' + \boldsymbol{V})' - F\boldsymbol{e}_r - \mu F\boldsymbol{e}_\theta, \tag{2}$$

where T is the tension, $\boldsymbol{V}$ is the shear force, $D(\ ) = \partial(\ )/\partial t$ with respect to the rotating reference frame, $(\ )' = \partial(\ )/\partial s$, $-F\boldsymbol{e}_r$ is the force per unit length of rod that the cylinder exerts on the rod in the direction normal to the cylinder (with F positive when this force is pointing inward), and μ is the coefficient of friction between the rod and the cylinder. Note that in the frictionless case the cylinder reaction force has only a component normal to the cylinder.

The total angular velocity of the rod element is given by

$$\boldsymbol{\Omega} = \omega_t\boldsymbol{R}' + \boldsymbol{R}' \times (D\boldsymbol{R}' + \omega\boldsymbol{k} \times \boldsymbol{R}'),$$

so that for a rod with a circular cross-section of radius a the angular momentum vector relative to the centre of mass of the element of mass $m\delta s$ at $\boldsymbol{R}(s,t)$ is

$$\boldsymbol{H}\delta s = \frac{1}{2}ma^2\delta s \left\{\omega_t\boldsymbol{R}' + \frac{1}{2}[\boldsymbol{R}' \times (D\boldsymbol{R}' + \omega\boldsymbol{k} \times \boldsymbol{R}')]\right\},$$

where $\omega_t\boldsymbol{R}'$ is the angular velocity of the rod element about the rod axis, and $\omega\boldsymbol{k}$ is the angular velocity of the rotating reference frame. Finally, the equation for the rate of change of angular momentum of the rod element is

$$D\boldsymbol{H} + \omega\boldsymbol{k} \times \boldsymbol{H} = (Q\boldsymbol{R}' + \boldsymbol{M})' + \boldsymbol{R}' \times \boldsymbol{V} - a\mu F\boldsymbol{k}, \tag{3}$$

where Q is the torque and $\boldsymbol{M}$ is the bending moment.

To these equations we add the following constitutive and constraint equations:

$$\boldsymbol{R}' \cdot \boldsymbol{R}' = 1, \tag{4}$$

$$\boldsymbol{R}' \cdot \boldsymbol{V} = 0, \tag{5}$$

$$\boldsymbol{M} = B(\boldsymbol{R}' \times \boldsymbol{R}''), \tag{6}$$

$$\boldsymbol{R}' \cdot \boldsymbol{e}_r = 0, \tag{7}$$

expressing, respectively, inextensibility, unshearability, linear elasticity in bending, and the cylindrical constraint.

3 Dimensional analysis

We now introduce the following dimensionless (barred) variables:

$$\begin{aligned} \tau = \omega t, \quad \bar{D} = \frac{\partial}{\partial \tau} \quad \bar{\boldsymbol{R}} = \frac{\boldsymbol{R}}{L}, \quad \bar{s} = \frac{s}{L}, \quad \varepsilon = \frac{a}{L}, \\ \bar{T} = \frac{TL^2}{B}, \quad \bar{F} = \frac{FL^3}{B}, \quad \bar{\boldsymbol{V}} = \frac{\boldsymbol{V}L^2}{B}, \\ \bar{Q} = \frac{QL}{B}, \quad \bar{\boldsymbol{M}} = \frac{\boldsymbol{M}L}{B}, \quad \bar{\boldsymbol{H}} = \frac{\boldsymbol{H}}{m\omega a^2}, \quad \bar{\omega_t} = \frac{\omega_t}{\omega}. \end{aligned} \tag{8}$$

L is a representative length such as the radius of the yarn package in unwinding or the radius of the casing in case of an oil drill pipe, or even the distance between the stabilisers.

As all variables will be dimensionless from now on, unless specifically stated otherwise, the barred notation will be dropped.

In terms of these dimensionless quantities the rate of change of linear and angular momentum equations (2) and (3) become

$$\Omega^2\{D^2\boldsymbol{R} + 2\boldsymbol{k} \times D\boldsymbol{R} + \boldsymbol{k} \times (\boldsymbol{k} \times \boldsymbol{R})\} = (T\boldsymbol{R}' + \boldsymbol{V})' - F\boldsymbol{e}_r - \mu F\boldsymbol{e}_\theta, \tag{9}$$

$$\varepsilon^2\Omega^2\,(D\boldsymbol{H} + \boldsymbol{k} \times \boldsymbol{H}) = (Q\boldsymbol{R}' + \boldsymbol{M})' + \boldsymbol{R}' \times \boldsymbol{V} - \varepsilon\mu F\boldsymbol{k}, \tag{10}$$

where

$$\Omega^2 = \frac{m\omega^2 L^4}{B} \tag{11}$$

measures the relative magnitude of the translational inertia terms.

In the case of a steel drill rod of radius 0.065 m rotating at say 2 Hz in a casing of radius 0.45 m, $\Omega^2 \approx 0.2$ and $\varepsilon^2 = 0.02$ so that it may be reasonable to neglect the rotary inertia terms relative to the translational inertia terms. Dimensions quoted here are compatible with the ranges of physical parameters quoted in [11]. We note, in this connection, that in the construction of one-dimensional rod theories for describing waves in elastic waveguides the unshearabillity assumption is consistient with neglecting the rotary inertia terms, and that although these assumptions are sufficient for low-frequency (long-wavelength) waves, at high frequencies and short wavelengths these effects become significant. See for example [5]. In the case of yarn twisting dynamics $\varepsilon \approx 10^{-3}$ [1, 3, 4].

4 Reduction of the problem: the equivalent oscillator

We now consider the steady-state problem so that $D(\ ) \equiv 0$, and in the light of the above discussion we neglect the rotary inertia. We will also assume that the force and moment loads at the remote ends of the rod are applied in the direction of the axis of the cylinder. These loads at both ends need not be co-axial and we shall assume that the loading device leaves the ends of the rod free to slide without friction ($\mu = 0$) along the circumference of the cylinder. Thus equations (9) and (10) reduce to

$$(T\boldsymbol{R}' + \boldsymbol{V})' = (F - \Omega^2 r)\,\boldsymbol{e}_r =: G\,\boldsymbol{e}_r, \tag{12}$$

$$(Q\boldsymbol{R}')' + \boldsymbol{M}' + \boldsymbol{R}' \times \boldsymbol{V} = \boldsymbol{0}, \tag{13}$$

where G is the effective reaction force and r is now the constant (dimensionless) radius of the cylinder. The constraint equations (4), (5), (7) are unchanged and $B = 1$ in the constitutive equation (6).

Equations (12), (13) can be simplified in several steps as follows. First form the scalar product of $\boldsymbol{k}$ with (12) and integrate to arrive at

$$(T\boldsymbol{R}' + \boldsymbol{V}) \cdot \boldsymbol{k} = P, \tag{14}$$

where P is the (dimensionless) applied end force. Next take the scalar product of $\boldsymbol{R}'$ with (13) to get $Q' = 0$, implying that the twisting moment Q is constant along the rod. An expression for the shear force is obtained by forming the vector product of $\boldsymbol{R}'$ with (13) and using (6):

$$\boldsymbol{V} = Q(\boldsymbol{R}' \times \boldsymbol{R}'') - [(\boldsymbol{R}'' \cdot \boldsymbol{R}'')\boldsymbol{R}' + \boldsymbol{R}'''] \,. \tag{15}$$

The formation of the scalar product of $\boldsymbol{R}'$ with (12), the use of $\boldsymbol{V}' \cdot \boldsymbol{R}' = -\boldsymbol{V} \cdot \boldsymbol{R}''$ (since $\boldsymbol{V} \cdot \boldsymbol{R}' = 0$) and (15) followed by integration gives an expression for the tension:

$$T = T_0 - \frac{1}{2}(\boldsymbol{R}'' \cdot \boldsymbol{R}''), \tag{16}$$

where T_0, the integration constant, is a reference tension (taken at one of the ends of the rod, for instance).

Because r is constant it follows from (1) that the position and (unit) tangent vectors can be written as

$$\boldsymbol{R} = r\cos\theta\,\boldsymbol{i} + r\sin\theta\,\boldsymbol{j} + z\,\boldsymbol{k}, \qquad \boldsymbol{R}' = r\theta'\,\boldsymbol{e}_\theta + z'\,\boldsymbol{k} = \sin\phi\,\boldsymbol{e}_\theta + \cos\phi\,\boldsymbol{k}, \tag{17}$$

where ϕ is the angle between the tangent of the rod and the axis of the cylinder. Substitution of (15), (16) and (17) into (14) gives

$$P = T_0\cos\phi - \frac{3}{2}\left[\frac{\sin^4\phi\cos\phi}{r^2} + \phi'^2\cos\phi\right] - (\cos\phi)'' + \frac{Q\sin^3\phi}{r}. \tag{18}$$

This equation can finally be integrated to arrive at an equivalent oscillator for the angle ϕ which can be written as

$$\frac{1}{2}\phi'^2 + V(\phi) = T_0, \tag{19}$$

with the 'potential energy' $V(\phi)$ given by

$$V(\phi) = P\cos\phi + \frac{K\sin\phi}{r} - \frac{Q\sin\phi\cos\phi}{r} - \frac{\sin^4\phi}{2r^2}, \tag{20}$$

where K is the (dimensionless) applied end moment. By differentiating (19) with respect to s we obtain an alternative form of (19):

$$\phi'' - P\sin\phi + \frac{K\cos\phi}{r} - \frac{Q\cos 2\phi}{r} - \frac{2\sin^3\phi\cos\phi}{r^2} = 0, \tag{21}$$

which is a generalisation of equation (2.41) in the paper by Coleman & Swigon [2] to the case of non-zero end loading.

If desired, all physical quantities, such as P, T, $\boldsymbol{V}$ and $\boldsymbol{M}$ can now be expressed in terms of the angle ϕ and its derivatives. A final quantity that will be useful later is the effective reaction force G for which we have, from (12),

$$G = (T\boldsymbol{R}'' + \boldsymbol{V}') \cdot \boldsymbol{e}_r. \tag{22}$$

5 Solutions and helical collapse

Fixed points of (19) are given by solutions of

$$V'(\phi) = 0, \tag{23}$$

and correspond to helical solutions with pitch angle $\pi/2 - \phi$ and axial wavelength λ given by

$$\lambda = \frac{2\pi r}{|\tan\phi|}. \tag{24}$$

By (17), the helix is right-handed if $0 < \phi < \pi/2$ or $-\pi < \phi < -\pi/2$, and left-handed if $\pi/2 < \phi < \pi$ or $-\pi/2 < \phi < 0$; it is in tension if $|\phi| < \pi/2$, and in compression if $\pi/2 < |\phi| < \pi$.

In the remainder of this section we shall only consider values of the integration constants that admit the straight rod, which has $\phi = 0$, as a solution. This means that we have to choose

$$Q = K. \tag{25}$$

The origin is then a saddle if $P > 0$ (straight rod in tension) and a centre if $P < 0$ (straight rod in compression).

Fig. 1 shows two phase portraits for the oscillator (19), subject to (25), taking $r = 1$, $K = 0.8$. Generically, the origin has two homoclinic orbits that connect the saddle to itself (as in Fig. 1(b)). These solutions correspond to asymptotically straight localised solutions. At special values of the parameters, however, a (heteroclinic) connection may be formed between the origin and a non-trivial saddle (as in Fig. 1(a)). Since this non-trivial saddle corresponds to a helix, these critical parameter values define loads at which the rod collapses into a helix. This is illustrated by the load-deflection diagram in Fig. 2 which shows the end shortening D, defined by

$$D = \int_{-\infty}^{\infty} (1 - \cos\phi(s))\, ds, \tag{26}$$

as a function of the applied load for one of the homoclinic orbits to the origin in Fig. 1(b)) (the one with $\phi > 0$). As the critical load $P_c = 0.1683$ is approached the rod coils up and D diverges. Right at P_c the solution is a pure (infinite) helix.

For sufficiently high P ($P > 0.3007$), indicated by the triangle in Fig. 2, the rod starts bending backwards on the cylinder over some arclength interval, i.e., z is no longer monotonic in s. This is quickly followed at higher P by self-intersection of the solution and therefore the dashed part of the curve in the figure is non-physical and will not concern us here (although it may mean that there is a 3D solution nearby; we make a comment on this in Section 7). Note though that there is a second critical load along the non-physical part of the curve at $P = 0.5123$. The corresponding left-handed helix is in compression at an angle $\phi = 2.1927$.

In [19] it is shown that there are at most two critical collapse loads, one of which leading to a self-intersecting solution and therefore non-physical. This non-physical collapse load exists for all values of K. The physical collapse load P_c of interest here only exists for $0 \le rK \le 0.9648$ and $1.9093 \le K/\sqrt{P} \le 2$, or, equivalently,

$$1.9093\sqrt{P} \le K \le \min\left\{0.9648/r, 2\sqrt{P}\right\}. \tag{27}$$

Fig. 3 gives a graphical representation of this condition. The angle ϕ of the critical helix varies between 0 ($K = 0$) and 0.7320 ($K = 0.9648$). This means the helix is always right-handed and

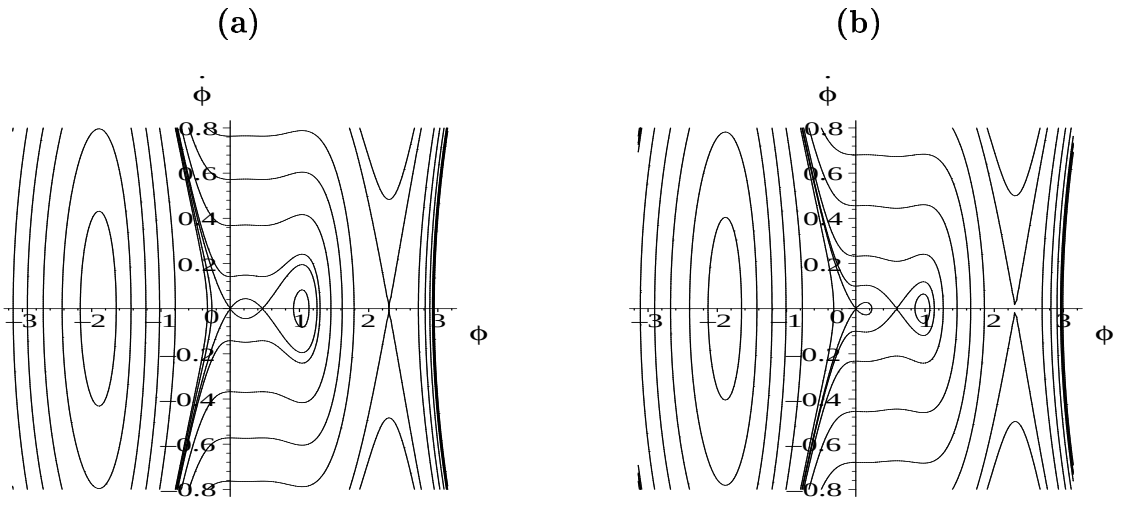

Figure 1: Phase-plane diagrams for the equivalent oscillator (19) subject to (25) for $r = 1$, $K = 0.8$ and (a) $P = P_c = 0.1683$, (b) $P = 0.1322$. Notice the saddle connection between the origin and the non-trivial fixed point at $\phi = 0.4660$ in (a).

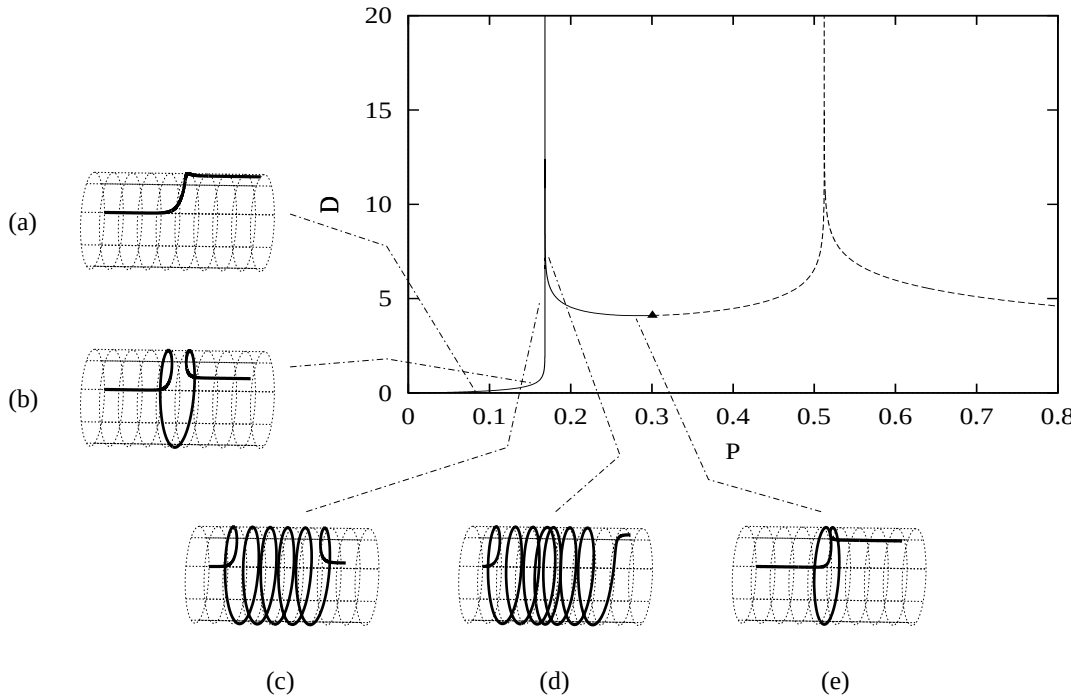

Figure 2: Load-deflection characteristic and evolution, under varying load P, of the asymptotically straight localised solution with initial $\phi > 0$ at $r = 1$, $K = 0.8$. There is a critical collapse load corresponding to a right-handed tensile helix at $P_c = 0.1683$. The triangle indicates where the rod starts to go backwards on the cylinder over some section of rod. This is soon followed by self-intersection, so the dashed part of the curve, including the second critical load at $P = 0.5123$, is non-physical. D is the dimensionless end shortening.

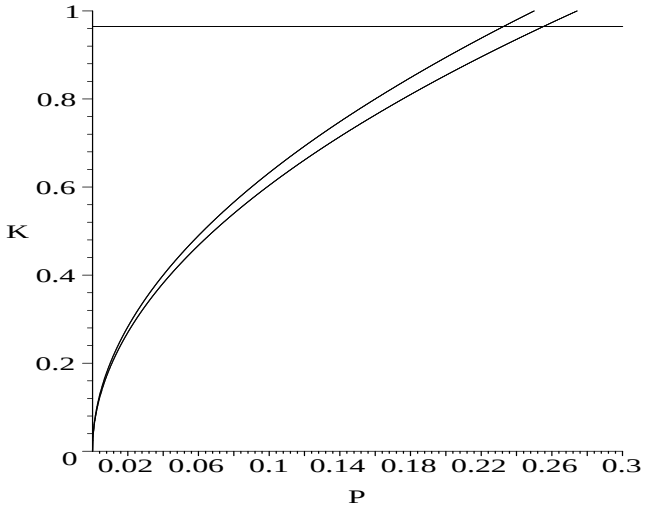

Figure 3: Region of helical collapse in the (P, K) end-load plane for $r = 1$. Collapse is only possible in the region enclosed by the three curves as given by the inequalities (27). Only the horizontal line depends on the radius r of the constraining cylinder. Where exactly in the region collapse occurs depends on r.

in tension. For the critical load of Fig. 1(a) the helix has an angle $\phi = 0.4660$ or $26.70°$. It then follows from (24) that the ratio of helical wavelength to radius is equal to 12.49. Non-critical helices of course are less constrained in their characteristics.

Fig. 4 shows the effective reaction force G for two different solutions along the load-deflection curve in Fig. 2. Here (a) and (c) are for a solution close to the collapse point. It is seen that G is constant over the central helical part of this solution and changes rapidly in the transition to the straight terminal sections where G tends to zero. For a rod inside a cylinder, as in the drill string problem, wall contact will be maintained as long as $F > 0$. Where F drops to zero the rod will lift off and the present model ceases to be valid. In terms of G the contact condition is $G > -m\omega^2 r$, so the critical lift-off level is set by the centrifugal force, and contact can always be preserved by using a sufficiently high driving frequency ω.

For a helical solution (22) and (21) yield relatively simple expressions for G and P:

$$G = \frac{\sin\phi\,(1-\cos\phi)\,(\sin\phi\,(1+\cos\phi) - rK)}{r^3}, \tag{28}$$

$$P = \frac{-rK(1-\cos\phi) + 2\sin^2\phi\,(rK - \sin\phi\cos\phi)}{r^2\sin\phi}. \tag{29}$$

We consider three special cases:

1. The straight rod: $\phi = 0$, $G = 0$, P and K indeterminate.

2. The (multi-covered) ring: $\phi = \pi/2$, $G = (1 - rK)/r^3$, $P = K/r$. So G drops to zero when the applied axial moment K provides the bending moment required to hold the rod in a ring of radius r.

3. The free helix: $G = 0$, $rK = \sin\phi\,(1+\cos\phi)$, $P = (\sin^2\phi)/r^2$. These are well-known relations for a Kirchhoff rod bent into a helix of radius r (see, e.g., [18]).

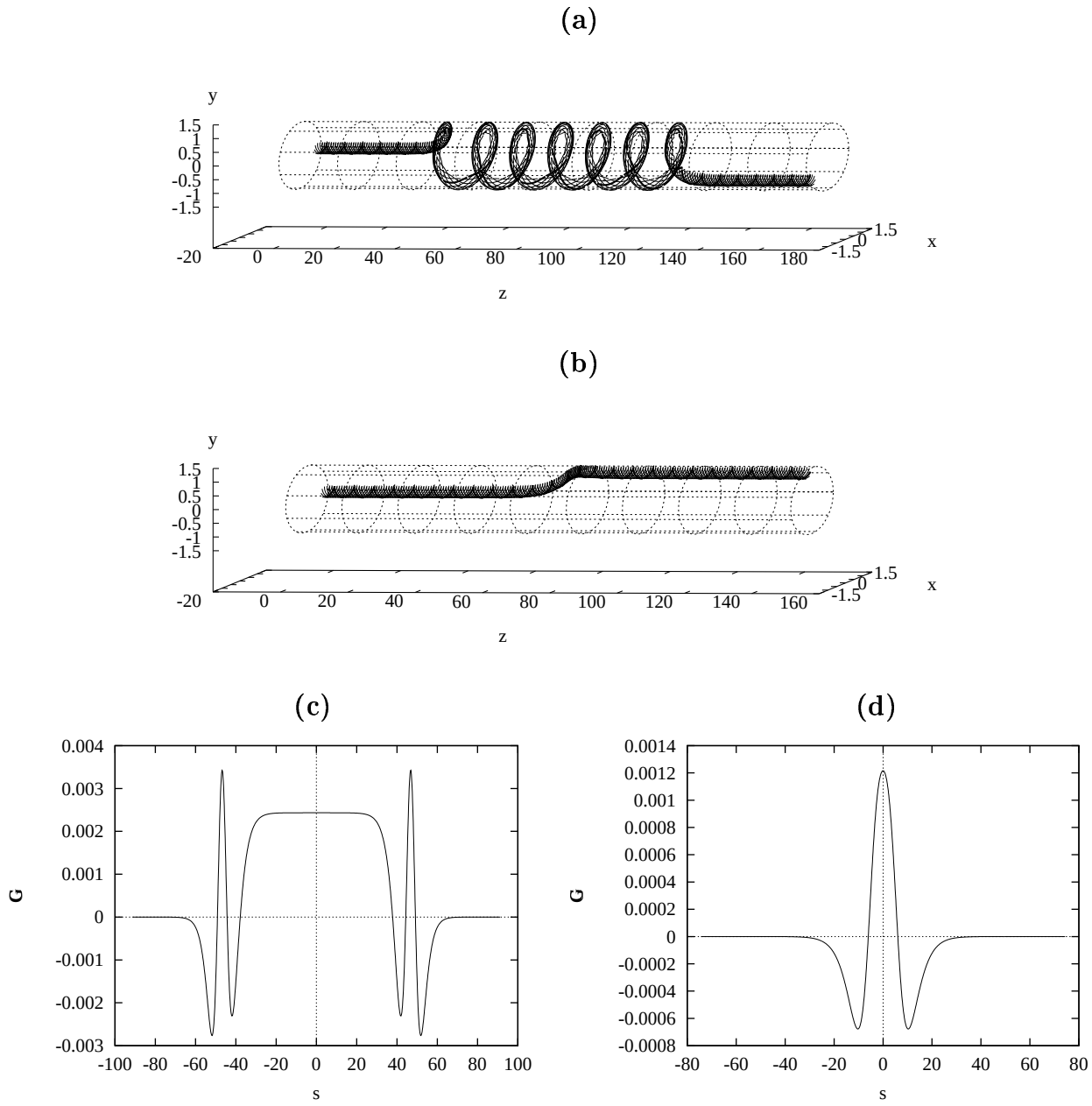

Figure 4: Physical shape and effective distributed reaction force G for (a,c) a localised solution close to $P_c = 0.1683$ ($D = 8.9036$) and (b,d) one at $P = 0.07111$ ($D = 0.05318$). Shown in the 3D diagrams are eight equally-spaced material lines of the rod (one emphasised) so as to illustrate the twist. ($r = 1,\ K = 0.8$.)

6 The balanced ply

In this section we look at a special type of solution called a balanced ply which is important in the textile spinning industry [7, 8, 13] and also in studies of DNA in molecular biology [2, 14, 15]. A ply consists of two segments of rod in continuous contact along a straight line, the ply axis. The ply is balanced if it carries no net forces and moments at its ends.

A balanced ply is a special case of a rod (more precisely, a pair of rods) winding on a cylinder of radius equal to the radius of the rod, one segment providing the required pressure force G to a 180-degrees rotated copy of itself. Indeed, if we set the applied end force P and the applied end moment K to zero, then (21) reduces to the balanced ply equation derived in [2] (the authors actually call it the equation for a generalised helix, i.e., a configuration with constant radius r and variable angle ϕ). This equation in turn has the uniform (right-handed) balanced ply with constant ϕ studied in [7, 8] as a special fixed-point solution:

$$Q\cos 2\phi + \frac{2}{r}\sin^3\phi\cos\phi = 0. \tag{30}$$

This equation can be interpreted as a formula for the twisting moment Q in terms of the ply angle ϕ. All other forces and moments are then also functions of ϕ, viz.

$$V = \frac{Q}{2r}, \qquad -T = rG = V\tan\phi, \qquad M = \frac{\sin^2\phi}{r}, \tag{31}$$

where $\boldsymbol{V} = V\boldsymbol{b}$ and $\boldsymbol{M} = M\boldsymbol{b}$, with $\boldsymbol{b} = \boldsymbol{R}'\times\boldsymbol{R}''/|\boldsymbol{R}''|$ the binormal of the helical rod. Note that the total twisting moment in the rod has the opposite sense to that of the space torsion of the helix, i.e., the sense the rod is winding about the ply axis. Also note that for small angles $G < 0$, so the two strands in the ply are repelling each other.

In further analysing (30) we observe that this equation remains invariant under the transformation $\phi \to \pi - \phi$, $Q \to -Q$, so if we restrict attention to right-handed plies we can assume $\phi \in [0, \pi/2]$ (a left-handed ply of the same angle is obtained for opposite Q). A graphical analysis reveals that there is a unique solution for $\phi \in [0, \pi/2]$ for any non-zero Q, a saddle $\phi_s \in [0, \pi/4]$ for $Q < 0$ and a centre $\phi_c \in [\pi/4, \pi/2]$ for $Q > 0$. In particular, this means that the balanced ply phase portrait does not contain a heteroclinic orbit, so a balanced ply does not collapse. The solution ϕ_s tends to 0 as $rQ \to 0$, and to $\pi/4$ as $rQ \to -\infty$, while ϕ_c tends to $\pi/2$ as $rQ \to 0$, and to $\pi/4$ as $rQ \to \infty$.

Curiously, this angle $\pi/4$ is exactly the maximum possible angle, ϕ_m, a uniform (i.e., helical) ply can have, larger angles leading to self-penetration of the rod. This follows from the lock-up condition quoted in a recent article by Stasiak & Maddocks [12]. Specifically, for a general double helix the authors give the lock-up condition $p/\rho = 2\pi$, where ρ is the radius and p the pitch, i.e., the period, of one of the helical strands. For our balanced ply $\rho = r$, and the condition leads to the lock-up angle $\phi_m = \pi/4 = 0.7853....$ Incidentally, for a single helix the authors in [12] give the lock-up condition $p/\rho = 2.512$, which, still using $\rho = r$, gives $\phi_m = 1.1905$ (68.21°), considerably larger than for a double helix.

7 Discussion

We have given the general formulation of an isotropic rod deforming on a rigid cylinder using the geometrically exact theory of rods, and shown that for such a rod whirling on a cylinder and

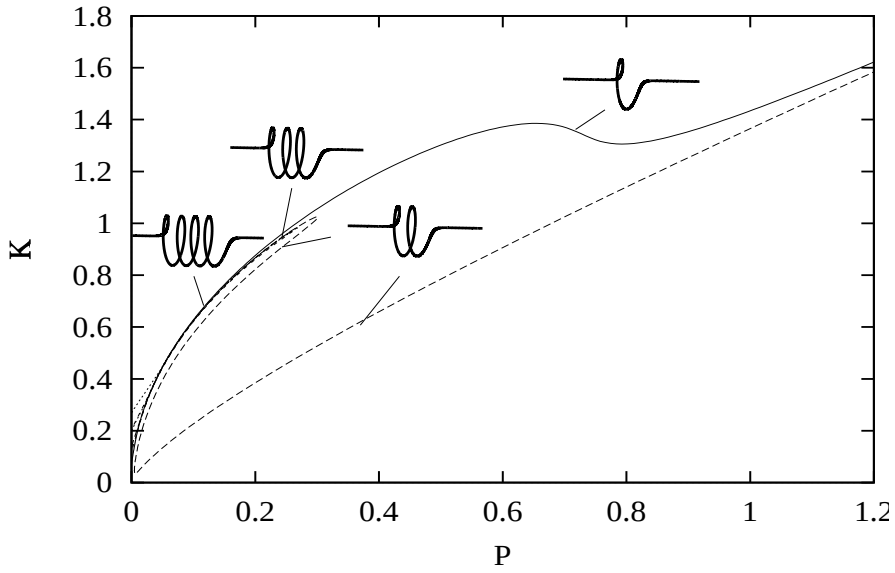

Figure 5: End-load curves for the first four co-axial solutions ($r = 1$).

subject to an end tension and an end moment satisfying certain conditions a helical collapse may occur. Apart from this physical collapse into a tensile helix we have also found a collapse into a compressive helix. This collapse, which occurs for a wider range of parameters, requires self-intersections and is therefore non-physical. This situation is similar to the case of looped solutions in planar Euler buckling. In such cases (as, for instance, in [9]) the problem of self-intersections is frequently discounted, it being argued that 'slightly three-dimensional' nearby states exist arbirarily close to those with self-intersecting loops. A similar situation may apply in our case.

The ends of the localised solutions need not be co-axial; indeed they rotate relative to each other in the loading process as can be seen in Fig. 2. Co-axial solutions, making an integer number of helical turns, therefore exist at isolated values of P. By using K as a second continuation parameter we can draw curves of such solutions in the (P, K) load plane; see Fig. 5. The 1-turn solution curve has two limit points in K and none in P. The 2-turn solution curve forms two limit points in both parameters. Associated with these pairs of limit points are hysteresis loops with jumps in the parameters. All n-turn solutions with $n > 2$ have only one limit point defining maximum loads able to support the particular solution. Note that as n increases the solution exists over a smaller and smaller range of loads about the collapse point (cf. Fig. 3). The curves in Fig. 5 are therefore seen increasingly to approach the collapse region of Fig. 3.

These (infinitely long) co-axial solutions give good approximations to shapes of sufficiently long rods held by quasi-stationary clamps. Sufficiently long here means longer than the length of rod needed in the helical turns, which depends on how close to critical the end loads are. A measure of this distance to criticality is provided by n, and recalling formula (24) for the helical wavelength and the fact that the end shortening of the rod forming the helix is given by $D = (1 - \cos\phi)L$, we can estimate

$$L > \frac{2\pi r n}{\sin\phi},$$

where ϕ is a function of r and the end loads P and K through (21).

Although our work does not give information on the stability of the solutions considered, the presence of the cylindrical constraint is expected to make a number of them stable and therefore observable in practice. We can again refer to studies of constrained Euler buckling for examples in which constraints are found to stabilise certain branches of solutions (see [9] and references therein). It would be interesting to use variational methods to investigate the stability of the helical and localised solutions in the present model; this will be pursued elsewhere.

We finally mention that the analysis presented in this paper can be extended to the case of a rod of non-symmetric cross-section. However, since one has to keep track of the orientation of the cross-section a director formulation as employed in [19] is required which complicates matters. It is also no longer possible to reduce the system of equations to a planar oscillator as in Section 4. Instead, one gets so-called spatial chaos with infinitely many localised solutions including multi-pulse ones. For more on this the reader is referred to [20].

References

[1] J.D. Clark, W.B. Fraser & D.M. Stump, Simulation of tension in yarn package unwinding, *J. Engng Math.* (in the press).

[2] B.D. Coleman & D. Swigon, Supercoiled configurations with self-contact in the theory of the elastic rod, *J. Elasticity* (in the press).

[3] W.B. Fraser, On the dynamics of the two-for-one twister, *Proc. Roy. Soc. Lond. A* **447**, 409-425 (1993).

[4] W.B. Fraser, Air drag and friction in the two-for-one twister: results from the theory, *J. Textile Inst.* **84**, 364-375 (1993).

[5] W.B. Fraser, Stress wave propagation in rectangular bars, *Int. J. Solids Struct.* **5**, 379-397 (1969).

[6] W.B. Fraser, D.M. Stump, Yarn twist in the ring-spinning balloon, *Proc. Roy. Soc. Lond. A* **454**, 707-723 (1998).

[7] W.B. Fraser & D.M. Stump, The equilibrium of the convergence point in two-strand yarn plying, *Int. J. Solids Struct.* **35**, 285-298 (1998).

[8] W.B. Fraser & D.M. Stump, Twist in balanced-ply structures, *J. Textile Inst.* **89**, 485-497 (1998).

[9] P. Holmes, G. Domokos, J. Schmitt & I. Szeberényi, Constrained Euler buckling: an interplay of computation and analysis, *Comput. Methods Appl. Mech. Engrg* **170**, 175-207 (1999).

[10] N.C. Huang & P.D. Pattillo, Helical buckling of a tube in an inclined wellbore, *Int. J. Non-linear Mech.* **35**, 911-923 (2000).

[11] J.D. Jansen, Non-linear rotor dynamics as applied to oilwell drillstring vibrations, *J. Sound Vibr.* **147**, 115-135 (1991).

[12] A. Stasiak & J.H. Maddocks, Best packing in proteins and DNA, *Nature* **406**, 251-253 (20 July 2000).

[13] D.M. Stump & W.B. Fraser, On the dynamical theory of twist in yarn plying, *Math. Engng Ind.* **7**, 41-56 (1998).

[14] D.M. Stump, W.B. Fraser & K.E. Gates, The writhing of circular cross-section rods: undersea cables to DNA supercoils, *Proc. Roy. Soc. Lond. A* **454**, 2123-2156 (1998).

[15] D.M. Stump & W.B. Fraser, Multiple solutions for writhed rods: implications for DNA supercoiling, *Proc. Roy. Soc. Lond. A* **456**, 455-467 (2000).

[16] X.C. Tan & P.J. Digby, Buckling of drill string under the action of gravity and axial thrust, *Int. J. Solids Struct.* **30**, 2675-2691 (1993).

[17] R.W. Tucker & C. Wang, An integrated model for drill-string dynamics, *J. Sound Vibr.* **224**, 123-165 (1999).

[18] G.H.M. van der Heijden, J.M.T. Thompson, Helical and localised buckling in twisted rods: a unified analysis of the symmetric case, *Nonlinear Dynamics* **21**, 71-99 (2000).

[19] G.H.M. van der Heijden, The static deformation of a twisted elastic rod constrained to lie on a cylinder, *Proc. Roy. Soc. Lond. A* (in the press).

[20] G.H.M. van der Heijden, A.R. Champneys & J.M.T. Thompson, Spatially complex localisation in twisted elastic rods constrained to a cylinder (to be submitted).